The C-terminus of connexin43 adopts different conformations in the Golgi and gap junction as detected with structure-specific antibodies

Gina E. SOSINSKY*†[1], Joell L. SOLAN‡, Guido M. GAIETTA*, Lucy NGAN*, Grace J. LEE*, Mason R. MACKEY* and Paul D. LAMPE‡

*National Center for Microscopy and Imaging Research, Center for Research in Biological Systems, University of California, San Diego, La Jolla, CA 92093-0608, U.S.A., †Dept. of Neurosciences, University of California, San Diego, La Jolla, CA 92093-0608, U.S.A., and ‡Molecular Diagnostics Programme, Division of Public Health Sciences, Fred Hutchinson Cancer Research Center, Seattle, WA 98109, U.S.A.

The C-terminus of the most abundant and best-studied gap-junction protein, connexin43, contains multiple phosphorylation sites and protein-binding domains that are involved in regulation of connexin trafficking and channel gating. It is well-documented that SDS/PAGE of NRK (normal rat kidney) cell lysates reveals at least three connexin43-specific bands (P0, P1 and P2). P1 and P2 are phosphorylated on multiple, unidentified serine residues and are found primarily in gap-junction plaques. In the present study we prepared monoclonal antibodies against a peptide representing the last 23 residues at the C-terminus of connexin43. Immunofluorescence studies showed that one antibody (designated CT1) bound primarily to connexin43 present in the Golgi apparatus, whereas the other antibody (designated IF1) labelled predominately connexin43 present in gap junctions. CT1 immunoprecipitates predominantly the P0 form whereas IF1 recognized all three bands. Peptide mapping, mutational analysis and protein–protein interaction experiments revealed that unphosphorylated Ser^{364} and/or Ser^{365} are critical for CT1 binding. The IF1 paratope binds to residues Pro^{375}–Asp^{379} and requires Pro^{375} and Pro^{377}. These proline residues are also necessary for ZO-1 interaction. These studies indicate that the conformation of Ser^{364}/Ser^{365} is important for intracellular localization, whereas the tertiary structure of Pro^{375}–Asp^{379} is essential in targeting and regulation of gap junctional connexin43.

Key words: confocal microscopy, connexin, electron microscopy, gap junction, membrane protein structure, phosphorylation, trafficking.

INTRODUCTION

Gap junction assembly and degradation is a rapid and highly regulated process and one that is critical to the functionality of a cell [1]. Gap junctions play a dynamic role in developmental regulation, ionic transmission, signal transduction pathways and metabolic co-operation. Specifically, gap junction structures are critical in co-ordinating responses, regulation of cell ensembles, helping to synchronize the action of neurons, transport of second messenger molecules and removal of secreted ions. Many distinct human diseases result from connexin mutations including hearing loss, cataracts, impaired nerve conduction and skin abnormalities (see current reviews [2–4]). The majority of these disease-related defects are site-specific mutations that result in misfolding or mistrafficking of connexins. For example, nine different Cx32 (connexin32) mutations associated with CMTX (X-linked Charcot-Marie-Tooth disease) cause either no protein expression or aberrant cellular localization [5].

Cx43 (connexin43) is the most ubiquitous connexin with widespread tissue expression, and many of the major steps in the Cx43 life cycle have been characterized. Connexins typically have a relatively short half-life ($\sim$1.5–5 h, with specific times depending on the connexin and cell type; [6]). The short connexin half-life is a key element of coupling regulation as it allows very dynamic and acute changes in gap junction regulation and GJC (gap junctional communication) [1,7]. For Cx43, oligomerization of the monomer into a hexamer (connexons) occurs in the TGN (*trans*-Golgi network) [8] and connexons are then moved by vesicles for insertion into the plasma membrane [9–11]. Connexons are hypothesized to migrate to cell–cell contact areas where they dock with a partner connexon in an adjoining cell and add to the edges of a plaque [9,10] or create a new plaque [12]. However, another mechanism for connexon delivery directly to junctional areas has recently been proposed [13]. The gap-junction plaques are then internalized as either whole plaques (annular junctions) or as vesicles for lysosomal and/or proteosomal degradation. What is not known is how the movement of each particular Cx43 species (monomer, hexamer, dodecamer and degradation product) is controlled during its life cycle, although unspecified phosphorylation events have been implicated [14,15].

Phosphorylation of Cx43 can regulate the kinetics of Cx43 trafficking, assembly, gating and turnover in a cell-cycle-stage-specific manner. In unstimulated NRK (normal rat kidney) cells, Cx43 isolated from immunoprecipitated cell lysates shows three bands on Western blots [15] with approximate molecular masses of 42, 44 and 46 kDa often referred to as the P0, P1 and P2 forms of Cx43. Treatment of cell lysates with alkaline phosphatase causes loss of the 44 and 46 kDa bands with a commensurate increase in the 42 kDa species, indicating that phosphorylation is responsible for the migration shift. However, this phosphorylation-dependent shift in migration is not simply due to the addition of the mass of phosphate (80 Da). Instead, there are probably specific phosphorylation events that can induce a conformational change in Cx43 that is detectable in SDS/PAGE. For example, it has been shown that phosphorylation on some combination of Ser^{325}, Ser^{328} or Ser^{330} is necessary to form the P2 isoform [16]. Since the P2 isoform has been shown to be present in gap-junction plaques [15], phosphorylation at these sites appears to induce a conformational

Abbreviations used: BFA, brefeldin A; Cx, connexin; Cy5, indodicarbocyanine; DAPI, 4′,6-diamidino-2-phenylindole; EM, electron microscopy; GST, glutathione transferase; MDCK, Madin–Darby canine kidney; NRK, normal rat kidney; PKC, protein kinase C; TGN, *trans*-Golgi network.

[1] To whom correspondence should be addressed (email gsosinsky@ucsd.edu).

change that allows inclusion in the gap-junction plaque and is detectable by the migration shift. Conversely, phosphorylation on Ser^{368} can be detected on the P0 isoform [17], thus gel electrophoresis cannot discern this event, though it has dramatic effects on channel selectivity [18].

Clearly the conformation of proteins can be regulated via phosphorylation to affect subcellular localization and protein–protein interactions. In addition, antibodies can be specific for distinct antigen conformations [19]. In the present study, we examined the binding properties of two anti-Cx43 monoclonal antibodies, CT1 and IF1, which were made to the same 23-amino-acid C-terminal peptide immunogen, but discerned distinct tertiary Cx43 structures found in different subcellular locales. We used a combination of epitope mapping experiments, immunolabelling and correlative light and electron microscopy to show that these antibodies are detecting distinct conformations of the C-terminus in the Golgi apparatus (CT1) and the plasma membrane (IF1). We show that the CT1 antibody detects a conformation which is influenced by phosphorylation on specific serine residues, whereas the IF1 antibody detects a phosphorylation-independent conformation important for protein–protein interactions.

MATERIALS AND METHODS

Antibodies

The anti-GST (glutathione transferase), Cx43CT1 (where CT is C-terminus), Cx43IF1, Cx43NT1 (where NT is N-terminus) and mouse monoclonal antibodies were made at the Hutchinson Center's Antibody Development Shared Resource and are available on a cost recovery basis from the Fred Hutchinson Cancer Research Center (http://www.fhcrc.org/science/shared_resources/antibody_development/products/connexins/). Cx43IF1 was named as such because it performs well in immunofluorescence and can immunoprecipitate Cx43 effectively but does not perform well in a Western immunoblot. To avoid confusion of the Cx43CT1 antibody with GST–Cx43CT constructs, we refer to these antibodies as CT1, IF1 and NT1. GST protein or peptides corresponding to rat Cx43 residues 1–20 (NT1) and residues 360–382 (CT1 and IF1) synthesized with a C-terminal or N-terminal cysteine respectively, for linkage to KLH (Keyhole Limpet haemocyanin) were used for immmunization as previously described [17]. Residues 360–382 are identical for rodent and human Cx43. The anti-Cx43 polyclonal antibody C6219, purchased from Sigma–Aldrich, was generated using a synthetic peptide corresponding to the C-terminal segment of the cytoplasmic domain (amino acids 363–382 with N-terminally added lysine). The anti-ZO-1 and Cx43 (13–8300) monoclonal antibodies were purchased from Zymed/Invitrogen. The latter antibody primarily recognizes the P0 band and was raised against a C-terminal peptide (amino acids 360–376). The anti-giantin polyclonal antibody was purchased from Covance Research Products.

Cell lines and culture conditions

All culture reagents were obtained from Gibco BRL, Life Technologies. MDCK (Madin–Darby canine kidney), NRK cells or Rat1 fibroblasts were grown at 37 °C in DMEM (Dulbecco's modified Eagle's medium) supplemented with 10 % FBS (fetal bovine serum), 100 units/ml penicillin, 100 mg/ml streptomycin and 2 mM glutamine and aerated with 5 % CO_2. MDCK cells were used to create stable lines expressing WTCx43 (where WT is wild-type) or Cx43 with serine to alanine mutations at Ser^{364} or Ser^{365}. Site-directed mutagenesis was performed using the GeneTailor site-directed mutagenesis kit (Invitrogen) on Cx43 ligated into pIREShyg (Clontech). Cells were transfected using an Amaxa Nucleoporator, selected with 200 μg/ml hygromycin and colonies were isolated using cloning rings. HeLa cells stably expressing a serine to alanine mutation at Ser^{368} have been described previously [17].

Peptide constructs

The Cx43 sequence encoding for the C-terminal amino acids 236–382 of Cx43 was cloned into a pGEX-2TK vector to generate GST–Cx43CT. C-terminus deletion/truncation constructs Δ6S (missing amino acids 364–373), T374 (missing amino acids 375–382) and T379 (missing amino acids 380–382) were all cloned into the pGEX-2T vector to generate the respective GST deletion constructs [20]. In addition, a C-terminal construct with Pro^{375} and Pro^{377} mutated to phenylalanine residues (denoted as P375/7F) was also cloned in the same manner. GST constructs were transformed into DH5α *Escherichia coli*, and GST fusion proteins were expressed and purified on glutathione–agarose. For CT1 epitope mapping, fusion proteins were run on SDS/PAGE (10 % polyacrylamide gel), blotted on to nitrocellulose and probed with a monoclonal anti-GST antibody (IgG2b) and the CT1 antibody (IgG2a), then visualized with a fluorescent dye-labelled isotype-specific secondary antibody [Alexa Fluor® 680 goat anti-mouse IgG2b (Molecular Probes) and IRDye800 donkey anti-mouse IgG2a (Rockland Immunochemicals), both extensively cross-reacted against other species] and directly quantified using the Li-Cor Biosciences Odyssey infrared imaging system and associated software. All quantifications of gel densitometry are based on three to five independent measurements. For IF1 epitope mapping, a pulldown approach was utilized. IF1 antibody (IgG_{2a}) and GST fusion proteins bound to glutathione–agarose were incubated in 1 % (v/v) Triton X-100 and 1 % (w/v) BSA in PBS at 4 °C for 1 h. Beads were washed three times in the same buffer and run on SDS/PAGE for Western blot analysis. Blots were incubated with an anti-GST antibody, then visualized with Alexa Fluor® 680 goat anti-mouse IgG2b to detect the deletion constructs and IRDye800 donkey anti-mouse IgG_{2a} to detect IF1 antibody that bound to the deletion constructs.

ZO-1 pulldown assays were performed by incubating fusion proteins bound to glutathione–agarose with NRK cell lysates in the presence of 1 % (w/v) BSA. Cells were lysed in PBS containing 0.5 % Triton X-100, 0.5 % deoxycholate, 50 mM NaF, 500 μM Na_3VO_4, 2 mM PMSF and 1× complete protease inhibitors (Roche Diagnostics), followed by centrifugation at 13 000 ***g*** at 4 °C for 10 min. Beads were washed three times in PBS containing 0.5 % Triton X-100 and 0.5 % deoxycholate, run on SDS/PAGE and blotted on to nitrocellulose. Blots were cut in half to separate GST fusion proteins from the ZO-1 migratory position. The lower half of the blot was probed with a monoclonal anti-GST antibody and the upper half of the blot was probed with a monoclonal anti-ZO-1 antibody. Blots were then incubated with IRDye800 donkey anti-mouse secondary antibody and directly quantified using the Li-Cor system.

Immunodetection of Cx43 from heart

Mouse studies were conducted under FHCRC Institutional Animal Care and Use Committee approval. Inbred mice (4 months of age in a FVB/N:C57BL6 background) were anaesthetized (avertin; 0.1 ml/3 g of body weight) and killed using cervical

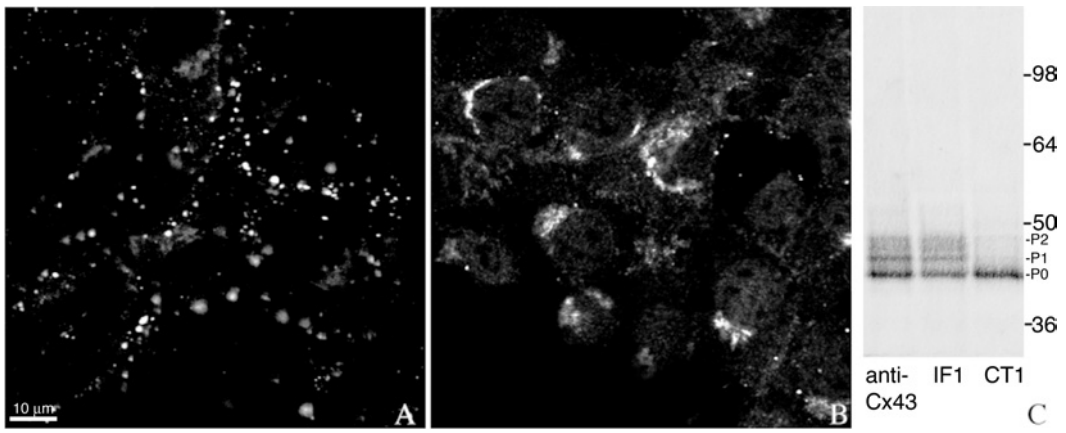

Figure 1 Different and specific subcellular localizations occur in unstimulated NRK cells with CT1 and IF1

NRK cells immunolabelled with (**A**) IF1 or (**B**) CT1 show punctate membrane labelling characteristic of gap junctional staining or intracellular labelling respectively. Cx43 was immunoprecipitated from NRK lysates with either a polyclonal antibody anti-Cx43 (Sigma), IF1 or CT1, separated by SDS/PAGE, Western blotted and probed with the NT1 antibody (**C**). CT1 recognizes only the lowest band, P0, whereas IF1 binds to all three bands, P0, P1, P2.

dislocation. Hearts were excised and placed either in ice-cold PBS for 30 s (control group) or incubated without coronary perfusion in non-oxygenated glucose-free PBS with 1.8 mM calcium at 37 °C. After 5, 15 or 30 min of incubation, hearts were longitudinally bisected and sonicated in Laemmli sample buffer with 50 mM NaF, 500 μM Na_3VO_4, 2 mM PMSF and 1× complete protease inhibitors for Western blot analysis [SDS/PAGE; (10 % gels)].

Peptide competition assays

Replicate lanes of recombinant GST–Cx43CT were blotted on to nitrocellulose, then probed with CT1 antibody alone or CT1 antibody plus 10 μg/ml of a peptide containing Cx43 residues 360–382 (pep360) or a peptide containing Cx43 residues 368–382 (pep368), then visualized using fluorescent-dye-labelled secondary antibody [IRDye800-conjugated donkey anti-mouse IgG (Rockland Immunochemicals)] and directly quantified using the Li-Cor system.

Alkaline phosphatase treatments

Cells were lysed with 0.2 % SDS in PBS, clarified by microcentrifugation and treated with 100 units/ml alkaline phosphatase at 37 °C for 30 min. Lysates were run on SDS/PAGE (10 % gel), blotted and co-incubated with CT1 (IgG2a) and NT1 (IgG1), then visualized with isotype-specific secondary antibodies [Alexa Fluor® 680 goat anti-mouse IgG2a (Molecular Probes) and IRDye800 donkey anti-mouse IgG1 (Rockland Immunochemicals)] and directly quantified using the Li-Cor system.

Immunofluorescence and confocal microscopy

Immunolabelling procedures followed those previously described in [21]. Fluorescence microscopy was performed using a BioRad MRC-1024 or an Olympus FluoView confocal microscope (Bio-Rad). Samples were labelled with secondary antibodies linked to FITC, Cy5 (indodicarbocyanine) or rhodamine (Jackson ImmunoResearch Laboratories). CT1, IF1, anti-calnexin and anti-giantin antibodies were used at 1:250 dilutions. Nuclei were labelled with DAPI (4′,6-diamidino-2-phenylindole) according to the manufacturer's instructions (Molecular Probes). All fluorescent secondary antibodies were used at a 1:100 dilution. It should be noted that we have observed microtubule-like staining in MDCK cells that do not express Cx43 using the CT1 antibody. This staining was not observed in NRK, HeLa or the same MDCK cells if they had been transfected with Cx43.

Immunoperoxidase staining and preparation of samples for EM (electron microscopy)

NRK cells were plated on MatTek dishes as described previously [21]. CT1 and IF1 labelling for EM was performed with a 1:250 dilution, whereas the goat anti-mouse HRP (horseradish peroxidase) conjugate was used at a dilution of 1:200. Cells were immunolabelled following a previously described protocol [22], fixed with 4 % (w/v) paraformaldehyde, 0.1 % glutaraldehyde in 1× PBS and reacted for 5–8 min in 0.05 mg/ml DAB (diaminobenzidine) with 0.01 % H_2O_2. After washing in 1× PBS, the labelled cells were fixed with 2 % glutaraldehyde in 1× PBS buffer for 20 min, washed five times with 1× PBS, post-fixed with 0.5 % osmium tetroxide in 1× PBS for 30 min and washed five times in double-distilled water. Cells were then dehydrated in an ethanol series and embedded in Durcupan ACM epoxy resin. Ultramicrotomy was performed using a Reichert Ultracut E ultramicrotome (Leica) and a diamond knife (Diatome U.S.) to produce 80–140 μm thick sections. Sections were collected on 50 mesh gilder copper grids. CT1 samples were stained en bloc with 2 % uranyl acetate overnight whereas IF1 sections were post-stained for 15 min in 2 % aqueous uranyl acetate. Transmission EM images were obtained with a JEOL JEM-1200EX electron microscope (JEOL U.S.A.) operating at 60 kV.

RESULTS

In the present study, we report on the binding properties of two monoclonal antibodies, CT1 and IF1, that were made to the same peptide representing the last 23 amino acids (360–382) of Cx43 but preferentially labelled different subcellular fractions of Cx43. In NRK cells, IF1 stained only gap-junction plaques whereas CT1 labelled mainly perinuclear Golgi-like structures (Figures 1A and 1B respectively). This perinuclear CT1 staining

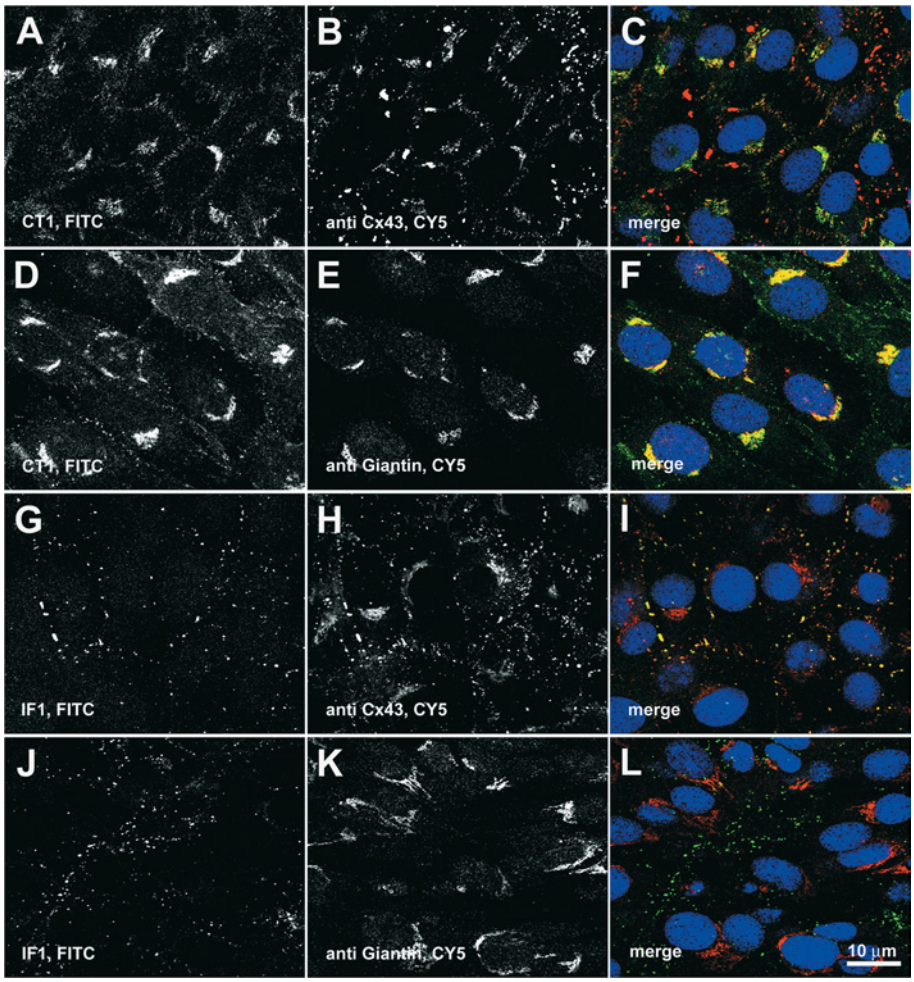

Figure 2 CT1 staining co-localizes with giantin, a Golgi marker, whereas IF1 staining is localized to gap-junction plaques

(**A**, **B**, **D**, **E**, **G**, **H**, **J** and **K**) Single-channel fluorescence images are shown in black and white (left-hand and middle columns) whereas the right-hand column contains the colourized overlay of the left-hand and middle panel images [FITC, green; Cy5, red; merge between the two colours will appear in yellow] along with DAPI counterstaining (blue) to mark cell nuclei (**C**, **F**, **I** and **L**). Strong co-localization of staining is shown between CT1 and anti-giantin (**D**–**F**), and IF1 and anti-Cx43 (**G**–**I**). CT1 co-stains poorly with junctional anti-Cx43 (**A**–**C**) and IF1 does not co-stain with anti-giantin (**J**–**L**).

was also seen in rat fibroblasts and MDCK cells expressing Cx43 (results not shown). We hypothesized that these antibodies bound to distinct Cx43 populations due to their recognition of conformationally distinct epitopes. In order to determine their specificity, we also tested the ability of these antibodies to immunoprecipitate Cx43 as compared with a polyclonal Cx43-specific antibody sold by Sigma that was generated against a similar peptide (amino acids 363–382). SDS/PAGE typically separates Cx43 into three macroscopic bands on a Western blot that correspond to different phosphorylated forms of Cx43 (called P0 or NP, P1 and P2). The Sigma antibody performs well in immunoblotting (recognizing all three isoforms) and immunofluorescence assays yielding apparent gap junctional and perinuclear localization [23].

Immunoprecipitations of Cx43 from NRK whole-cell lysates using IF1, CT1 or the Sigma antibody were detected using a Cx43 antibody to the N-terminus that detects all three phospho-isoforms (designated NT1). CT1 immunoprecipitated primarily the P0 form, whereas IF1 and the Sigma polyclonal antibody immunoprecipitated the P0, P1 and P2 forms (Figure 1C).

Co-localization studies with CT1 and IF1

In order to further address specific organellar localization, we performed double immunofluorescence labellings with either CT1 or IF1 and the Sigma polyclonal antibody anti-Cx43 (Figures 2A–2C) or a polyclonal antibody against giantin (Figures 2D–2F). Giantin is a membrane-bound component of the *cis* and medial Golgi [24] that has been shown to play a role in transport of vesicle-associated tethering factor [25]. We found that CT1 and Sigma polyclonal antibodies co-labelled intracellular structures in a perinuclear location (yellow in the merged image, Figure 2C; the CT1 staining is more intense than that of the Sigma antibody) but to a far less extent the punctate, gap junctional Cx43 (shown in red) present in the plasma membrane. This was also reflected in the Western blot in Figure 1(C) where the predominant species recognized by CT1 is P0, though very faint bands possibly co-migrating with the phosphorylated species were present. The CT1 labelling mainly co-localized with giantin (Figures 2D–2F; yellow in the merged image, Figure 2F). In the merged images (Figures 2C, 2F, 2I and 2L), DAPI staining (shown in blue) was included as a nuclear marker to help distinguish different cells.

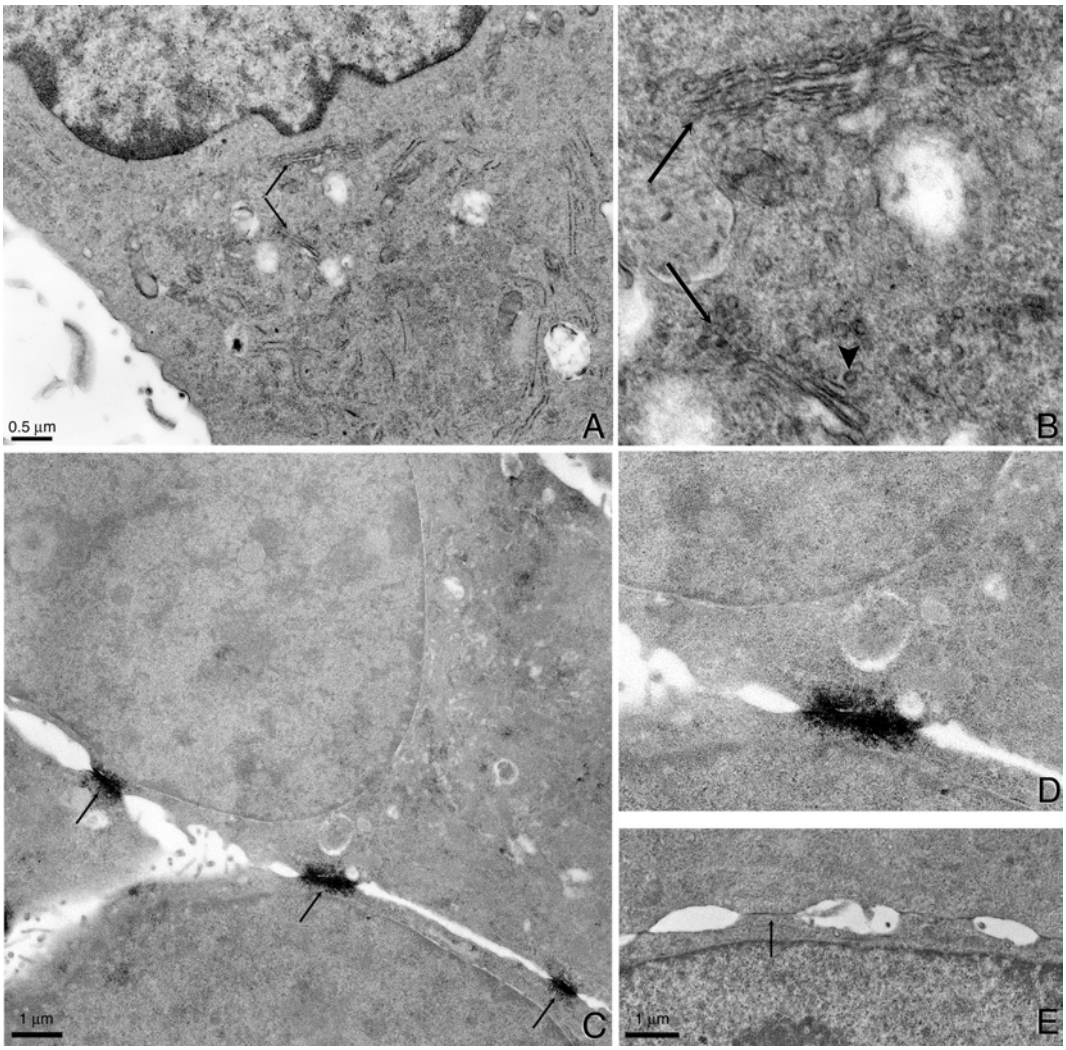

Figure 3 The CT1 epitope is found in the Golgi apparatus but is not required for Golgi entry

Immunoperoxidase labelling with CT1 in NRK cells shows an enhancement of staining in the Golgi apparatus region. (**A**) A low magnification image of the perinuclear region. The two arrows point to two regions of Golgi stacks that are shown at higher magnification in (**B**). The magnification in (**B**) is ~3.7 times that of (**A**). Note the overall staining of the Golgi stacks (arrows) as well as membrane staining in some vesicles (arrowhead). (**C**) Conversely, immunoperoxidase labelling with IF1 heavily stains gap junctions (arrows) without any significant intracellular labelling. (**D**) The 2× enlargement of the centre gap junction reveals small vesicles lying underneath the gap junction. (**E**) For comparison, NRK cells that have been CT1-immunoperoxidase-labelled reveal no significant gap junction staining (e.g. arrow).

Similar CT1 labelling patterns were found in Rat1 fibroblasts and Cx43-transfected MDCK cells indicating that localization in the Golgi apparatus is not cell-type-specific (results not shown). Conversely, IF1 staining overlapped significantly with that of the Sigma polyclonal antibody at apparent gap junctional structures (Figures 2G–2I; yellow in the merged image, Figure 2C) but did not overlap with that of the anti-giantin antibody (Figures 2J–2L).

Higher resolution subcellular localizations of CT1 to the Golgi apparatus and IF1 to gap-junctional plaques by EM

Localization at EM resolution allows us to look at the distribution of CT1 staining in the region of the cell containing the Golgi apparatus. When using CT1 with stronger fixation conditions than those used for light microscopy, immunoperoxidase methods provided the best sensitivity with minimum background [26]. Light microscopy of immunoperoxidase-stained samples showed similar staining patterns to the fluorescence images (results not shown). Figure 3(A) shows a low magnification electron microscopic view of the perinuclear area of the cell. The specimen has been counter-stained with uranyl acetate in order to visualize the cell components and this counter-staining accounts for the dark colour of the nucleus. This sample has good ultrastructural preservation particularly in the Golgi membrane stacks and small vesicles surrounding the Golgi apparatus. A higher (~3.7×) magnification view (Figure 3B) revealed uniform staining across the Golgi stacks (arrows) consistent with the confocal images in Figures 2(A) and 2(D). In addition some, but not all, of the trafficking vesicles in the Golgi region appear to be highlighted by the peroxidase reaction product (see example denoted by the arrowhead).

Immunoperoxidase methods using the IF1 antibody heavily stained gap-junction plaques with almost no intracellular staining (Figure 3C). Higher magnification of the centre gap junction (Figure 3D) revealed staining of small vesicles, which were presumably part of the degradation component of the connexin life cycle [9]. The immunoreactivity for IF1-labelled gap junctions is

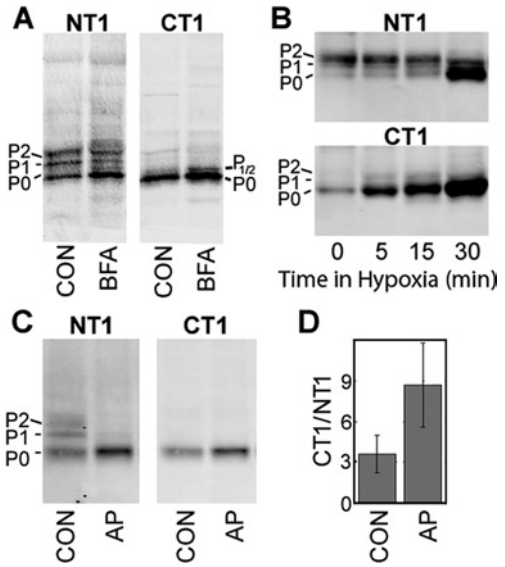

Figure 4 An increase in the amount of available epitope for CT1 binding occurs after BFA or alkaline phosphatase treatment and during hypoxia in heart

(**A**) NRK cells were treated with BFA or not (CON). Western blot analysis of cell lysates were performed using NT1 to detect total Cx43 (NT1 panel) and CT1-reactive Cx43. (**B**) Immunoblot analysis of lysates from mouse heart exposed up to 30 min of hypoxia and detected with an antibody to total Cx43 (NT1; top panel) and CT1 (bottom panel). (**C**) NRK cell lysates treated with alkaline phosphatase (AP) or not (CON). Blots were probed with both NT1 (left-hand panel) and CT1 (right-hand panel) to detect total Cx43. Signals from (**C**) were directly quantified and the ratio of CT1 to NT1 binding determined for three experiments (**D**). Protein loads were equalized in all lanes.

significantly heavier when compared with gap junction labelled with CT1, even with the more contrasting en bloc uranyl acetate counter-stain (Figure 3E, arrows). The contrast in the CT1-labelled gap junctions is primarily due to mass density and also to some slight specific staining that is also seen in the light microscopy images.

The CT1 epitope is present before Cx43 enters the Golgi apparatus

Since the CT1 epitope appeared to be enriched in the Golgi apparatus we examined whether this epitope was required for Golgi entry. To address this question, we treated NRK cells with BFA (brefeldin A), which results in Golgi disassembly. NRK cells were incubated with BFA for 5 h and whole cell lysates were run on SDS/PAGE, blotted and co-incubated with NT1 (IgG_1) and CT1 (IgG_{2a}) antibodies. Consistent with previous results from Laird et al. [12], the NT1 signal showed that BFA treatment resulted in enrichment of the 42 kDa or P0 isoform at the expense of the P1 and P2 forms and accumulation of a transiently phosphorylated 43 kDa isoform (Figures 4A and 4B, NT1; BFA lane labelled $P_{1/2}$). Probing of the same blot with the CT1 antibody showed that this antibody recognized only the 42 kDa and 43 kDa isoforms of Cx43 (Figure 4A, CT1) and that this signal was enriched upon BFA treatment (Figure 4A, CT1). Immunofluorescence of CT1- and IF1-stained BFA-treated samples was performed with a Cx43 polyclonal antibody or giantin antibody co-localizations (results not shown). These images demonstrated that the CT1 staining remained intracellular, with some perinuclear concentrations, but the fluorescence was more dispersed throughout the cytoplasm and did not entirely co-localize with giantin. Most plaques that had been stained with IF1 and the Cx43 polyclonal antibody appeared to have been internalized during the 5 h BFA protocol as previously reported [12]. Therefore these results indicate that the CT1 epitope occurs on Cx43 prior to its entry into the Golgi apparatus.

CT1 epitope increases in ischaemic heart

We and others have shown that in hypoxic heart, the SDS/PAGE migration of Cx43 shifts from slower-migrating isoforms to the P0 isoform and that this corresponds to a loss of gap-junction plaques at the intercalated disc [16]. We used the CT1 antibody to examine whether its binding would increase during mouse heart hypoxia. Hearts were incubated in non-oxygenated PBS for 0–30 min at 37 °C, lysed in SDS sample buffer, run on SDS/PAGE, blotted and probed with the CT1 and NT1 antibodies. The CT1 signal was increased by over 50 % (56 % $\pm$ 30.5 %) in as early as 5 min and increased to 6-fold (6.31 $\pm$ 2.47) over control levels by 30 min of ischaemia (Figure 4B). At the later time points, the CT1 signal increase clearly coincided with an increase in the P0 form of Cx43, consistent with the idea the CT1 senses a conformation of Cx43 that is not typically found in the slower-migrating isoforms of Cx43.

CT1 recognizes primarily the P0 form of Cx43

The Cx43 migration shift during hypoxia is a result of dephosphorylation on specific serine residues [16]. A similar migration shift was first shown by Musil et al. [14], by *in vitro* treatment of cell lysates with alkaline phosphatase, where the P1 and P2 bands of Cx43 are lost with a commensurate increase in the faster migrating P0 form (Figure 4C, AP lane). In order to further characterize how the phosphorylation status of Cx43 influences the binding of CT1, NRK whole cell lysates, treated with alkaline phosphatase, were run on SDS/PAGE, blotted and incubated with CT1 and NT1. In Figure 4(C), a Western blot of cell lysate (left-hand panel, CON lane) blotted with the NT1 antibody and detected with an IgG1-specific secondary shows the three Cx43 bands (P0, P1 and P2) as expected. Probing of the same blot with CT1 recognized only the P0 form (right-hand panel, CON lane). When NRK cell lysates were treated with alkaline phosphatase prior to SDS/PAGE, the NT1 signal showed Cx43 running exclusively as P0 (left-hand panel, AP lane) and the CT1 signal showed increased binding to P0 (right-hand panel, AP lane). Quantification of this blot (Figure 4D) indicated that the amount of available epitope that was recognized by CT1 increased more than 2-fold upon alkaline phosphatase treatment. This combined with the hypoxic heart results indicate that CT1 binds to a non-phosphorylated epitope that is biologically relevant during the heart tissue response to insult.

CT1 recognizes a sub-region of the C-terminus containing Ser^{364}/Ser^{365}

In order to determine the specific portion of the C-terminal peptide that formed the antigenic epitopes for IF1 and CT1, we performed epitope-mapping experiments using GST fusion constructs containing Cx43 deletions/truncations/substitutions and peptide competition. A graphic showing the sequence of the C-terminal peptide (pep360), a smaller peptide (pep368) and deletion constructs (Δ6S, T374 and T379) is shown in Figure 5(A). CT1 binding to these deletion constructs was determined by Western blot (Figure 5B) and then quantified after normalization to binding of an anti-GST antibody (Figure 5C). CT1 did not recognize a deletion construct missing residues 364–373. However,

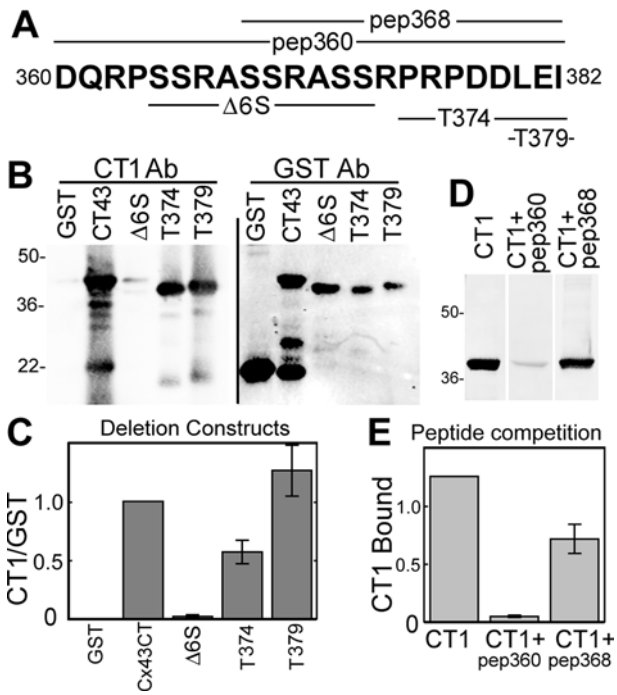

Figure 5 Epitope mapping of CT1 indicates that its epitope is localized to residues 364–368

A combination of GST fusion proteins expressing Cx43CT deletion/truncation mutants and peptide competition were used to determine the epitope recognized by CT1. (**A**) depicts the C-terminal amino acid sequence used to generate CT1 and IF1 (bold letters), the deleted portions of the fusion constructs (Δ6S, T374 and T379) and the amino acids present in the peptides (pep368 and pep360) used in the present experiments. Western blots were performed on the deletion/truncation constructs using CT1 and GST antibodies (**B**). (**C**) Signals were directly quantified and the ratio of CT1 to GST binding was determined ($n = 3$, $P < 0.001$ and $P < 0.05$ respectively; Student's t test values). Western blots were performed on GST–Cx43CT using CT1 alone, or in the presence of the immunizing peptide, pep360, or a peptide comprising amino acids 368–382, pep368 (**D**). (**E**) CT1 signal from experiments as shown in (**D**) were quantified and values in the presence of pep360 and pep368 were different from controls ($n = 3$, $P < 0.001$ and $P < 0.05$ respectively; Student's t test values). Taken together, the graphs in (**C**) and (**E**) indicate the primary epitope determinant is between amino acids 364–368.

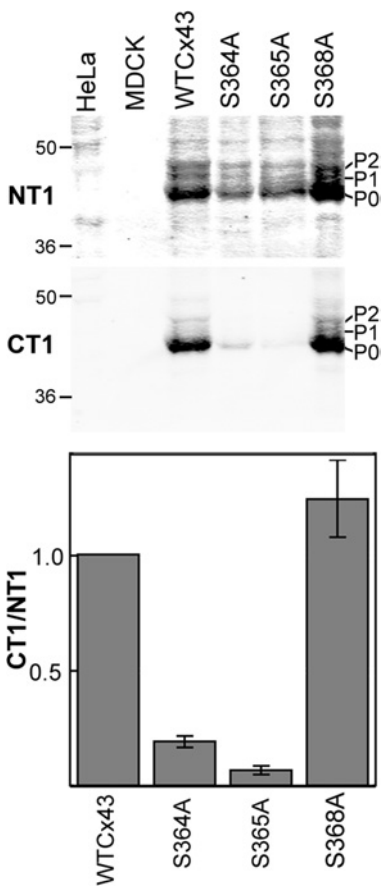

Figure 6 Mutation of either Ser^{364} or Ser^{365} affects CT1 antibody binding

WTCx43 or Cx43 containing serine to alanine mutations at residues Ser^{364}, Ser^{365} or Ser^{368} were transfected into either MDCK cells or HeLa cells. Western blot analysis was performed on lysates from cells expressing these constructs or the parental, Cx43-negative cells. Blots were incubated with NT1, to detect total Cx43, and CT1 (top panels). Signals were directly quantified and the ratio of CT1 to NT1 determined (bottom panel). Ser^{364} and Ser^{365} values were different from WTCx43 ($n = 5$ and $P < 0.001$, Student's t test values).

it recognized truncation constructs at amino acid residues 374 and 379 (Figure 5B). The 364–373 region contains three di-serine repeats, Ser^{364}/Ser^{365}, Ser^{368}/Ser^{369} and Ser^{372}/Ser^{373}. To further define the epitope, peptide competition experiments were performed, using the immunizing peptide, pep360, and a peptide containing residues 368–382 (Figure 5D). We found that pep360 was much more effective at inhibiting CT1 binding (10-fold inhibition) than pep368 (40 % inhibition), indicating that Ser^{364}–Ala^{367} is the primary epitope for the CT1 antibody (Figure 5E). Given the fact that CT1 primarily recognized the dephosphorylated form of Cx43, we hypothesize that non-phosphorylated Ser^{364} and/or Ser^{365} are critical features of the CT1 epitope.

To further confirm that Ser^{364} and Ser^{365} are a requirement for CT1 binding, full-length Cx43 was transfected into MDCK cells that do not natively express any Cx43 [27]. Cells containing unmodified Cx43 (WTCx43), Cx43 containing a serine to alanine substitution at Ser^{364} (S364A) and Cx43 with a serine to alanine mutant at Ser^{365} (S365A) were prepared. CT1 did not bind either of these mutants efficiently (Figure 6), indicating that serine residues at both of these positions were required for CT1 recognition. Even when there was faint recognition (as in the S364A lane) CT1 reacts with the P0 form only. To further determine that Ser^{368} was not influencing CT1 binding, HeLa cells stably expressing a serine to alanine mutation at Ser^{368} were also analysed (Figure 6). CT1 bound as well to S368A as to WTCx43. It should be noted that all of these mutants make predominantly the P0 form of Cx43. Figure 6 also shows that CT1 is specific for Cx43, as it did not react with HeLa or MDCK cell lysates that do not endogenously express Cx43. Taken together, these results indicate that CT1 recognizes the Cx43 fraction that has not been post-translationally modified at Ser^{364} and/or Ser^{365}.

IF1 recognizes a sub-region of Cx43 close to the end of the C-terminus

Epitope mapping for IF1 was performed slightly differently as it performs poorly in a Western blot. However, since IF1 is able to recognize Cx43 by immunoprecipitation, a pulldown approach was utilized. Glutathione-bead-immobilized GST fusion constructs were incubated with IF1 for 1 h, washed and run on SDS/PAGE. Western blots were performed using an anti-mouse antibody to detect IF1 (Figures 7A and 8A, top panels) and anti-GST to detect the GST proteins (bottom panel). Full-length GST–Cx43CT was the most efficient, followed by Δ6S and T379; T374 was particularly inefficient (Figure 7), pulling down 20-fold less IF1, whereas T379 pulled down 5-fold less (both significantly different from CT1, $P < 0.001$, Student's t test). Since deletion

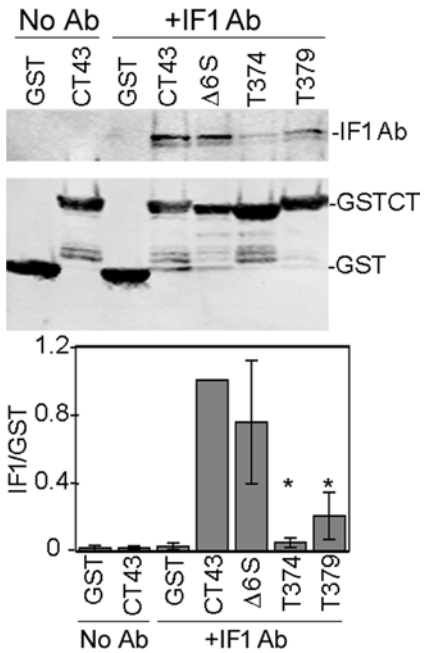

Figure 7 IF1 binding to deletion/truncation constructs indicates that the epitope is near the C-terminal end of the sequence of Cx43

GST fusion proteins expressing Cx43CT deletion/truncation mutants were incubated with IF1 and assessed for their ability to bind or pulldown the antibody. Fusion proteins immobilized on glutathione–agarose were either incubated with IF1 (+ IF1 Ab) or without (No Ab). Western blot analysis on these samples were performed using a monoclonal anti-GST antibody to detect the fusion proteins (bottom panel). IF1 was detected with the anti-mouse secondary antibody (top panel). Signals were directly quantified and the ratio of IF1 to GST signal determined (graph; $n = 5$ and $P < 0.001$, Student's t test values). $^*P < 0.001$ compared with the GST43 control. Ab, antibody.

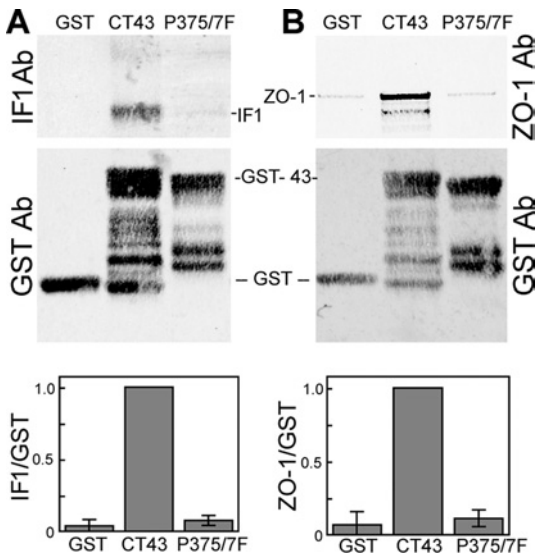

Figure 8 Pro^{375} and Pro^{377} are critical for IF1 binding and ZO-1 interaction with the C-terminus of Cx43

GST fusion proteins containing GST alone, Cx43CT or Cx43CT with Pro^{375} and Pro^{377} converted into phenylalanine residues were bound to glutathione–agarose and incubated with IF1 (**A**) or NRK cell lysates (**B**). After Western blotting of the samples, the membranes were cut to separate fusion proteins from the IF1 antibody or ZO-1 migratory positions. GST fusion proteins were probed with a monoclonal anti-GST antibody (**A** and **B**; GST Ab). Bound IF1 was directly detected using an anti-mouse secondary antibody (**A**; IF1 Ab). The upper portion of the blot in (**B**) was probed with a monoclonal anti-ZO-1 antibody (**B**; ZO-1Ab). Signals were directly quantified and the IF1 to GST ratio is presented in (**A**) ($n = 5$ and $P < 0.001$) and the ZO-1 to GST ratio in (**B**) ($n = 4$ and $P < 0.001$, Student's t test value). Ab, antibody.

of 372–373 or 379–382 did not affect binding (i.e. IF1 bound to the Δ6S and T379 deletion constructs; Figure 7A), it appears that the IF1 paratope binds primarily to the Cx43 region within residues 375–379 (Pro–Arg–Pro–Asp–Asp). To further define the role that the proline residues at 375 and 377 play, we performed a pulldown of IF1 antibody with Cx43 containing Pro^{375} and Pro^{377} mutated to phenylalanine residues. Mutation of these proline residues essentially eliminated IF1 binding to the fusion protein (Figure 8A) indicating that they are a key feature of the IF1 epitope. Given that IF1 binds to a conformation of Cx43 residing chiefly in apparent gap-junction plaques, we wondered whether Pro^{375} and Pro^{377} might be part of a conformation important for protein–protein interactions. We focused on ZO-1, a protein that requires at least the three C-terminal residues for binding to Cx43 [20,28]. Given the proximity of Pro^{375} and Pro^{377} to the C-terminus and the apparent specificity of IF1 for gap junctional structures, we hypothesized that these residues would influence ZO-1 binding. We again utilized a pulldown approach in which we incubated cell lysates from NRK cells with the GST fusion proteins immobilized on glutathione beads and ran the bound proteins on SDS/PAGE. Although GST–CT43 efficiently pulls down ZO-1, neither GST alone nor the Pro^{375}/Pro^{377} mutant bound ZO-1 (Figure 8B).

DISCUSSION

The C-terminus of Cx43 is critical for binding of cellular components such as ZO-1 [20,28–30] and tubulin [31] as well as binding to the intracellular loop of Cx43 [32]. An illustration of the flexible C-terminus as determined by NMR methods [33] is shown in Figure 9. Using two antibodies generated against a peptide comprising the C-terminal 23 amino acids of Cx43 (360–382), we have found that the C-terminus is present in at least two distinct conformations when present within gap-junction plaques or in cytoplasmic membranes.

The IF1 antibody epitope mapped to the amino acids P^{375}RPDD^{379} and required Pro^{375} and Pro^{377} for binding. In addition, staining with IF1 was found entirely in gap-junction plaques indicating that the conformation of P^{375}RPDD^{379} may be different from intracellular Cx43 species. Since proline residues often confer rigidity or a kink to tertiary structure, we focused on the role of proline residues in forming this epitope and hypothesized they might be able to regulate protein–protein interactions. This kink is reflected in the NMR structure shown in Figure 9 (region in the dotted-line box indicated by the arrow). The C-terminus of Cx43 has been shown to bind to the PDZ domain of ZO-1 in a manner dependent on the last three residues (Leu^{380}–Ile^{382}) of Cx43, and immunofluorescence studies indicate that the ZO-1 and Cx43 interaction occurs primarily at apparent gap junctional structures [20,28–30]. When we substituted phenylalanine residues for Pro^{375} and Pro^{377}, ZO-1 binding was lost. These results indicate that Cx43 localization to a gap junction implies a specific structural conformation at residues Arg^{374}–Asp^{379} that is also important for ZO-1 binding. Interestingly, another group has shown that this region of the C-terminus may play a role in regulation at the gap-junction plaque. Shibayama et al. [34] have identified a peptide that tightly bound the Cx43CT and induced shifting of residues 376–379 when examined by NMR. This peptide could inhibit gap junction uncoupling, increase the mean open time of channels and potentially affect the selectivity of the channel. Taken altogether, these results show that the conformation of residues

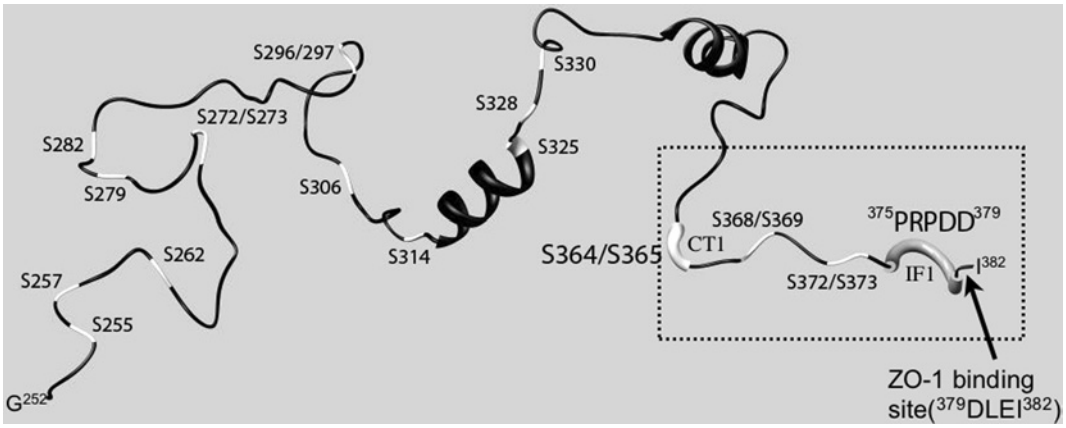

Figure 9 Cx43 sequence topology and possible C-terminal phosphorylation sites

Richardson diagram of the secondary structure of the Cx43CT amino acids 250–382 at low pH [49]. The serine residues are coloured white and labelled on the polypeptide chain. The thicker white segment indicates the region most likely forming the binding pocket for CT1, whereas the thicker grey tube would form the epitope for IF1 as determined by the results presented in the present study. The dotted-line box highlights the part of the structure that was used as the initial immunogen and the arrow points to the terminal amino acids that are important in ZO-1 binding.

$P^{375}RPDD^{379}$ is important for regulation of Cx43 in the gap-junction plaque and may have several functional consequences. Conversely, the conformations of Ser^{364} and Ser^{365} can apparently regulate the intracellular localization of Cx43 and binding of the CT1 antibody. The present study indicates that elimination of serine residues at either or both of these sites can affect the configuration of the C-terminus and that loss of the CT1 epitope is correlated with inclusion in a gap junction. Both Ser^{364} and Ser^{365} have been reported to be phosphorylated in response to increased cAMP levels which leads to increased trafficking of Cx43 to gap-junction plaques [35–37]. Thus it seems likely that phosphorylation of Ser^{364} and/or Ser^{365} is the modification that eliminates the CT1 epitope in cells and that this event is correlated with gap-junction formation. Regulation of the CT1 epitope appears to occur after or upon Golgi exit as treatment of cells with BFA, which results in the loss of P1and P2 and the appearance of a phosphatase-sensitive band migrating just above the P0 form [12,38] (Figure 4A, $P_{1/2}$), showed that both P0 and $P_{1/2}$ were CT1 reactive, indicating that the CT1 epitope is present prior to Golgi entry. It is interesting to note that an antibody from Zymed (13-8300), like the CT1 antibody, has been reported to bind primarily to non-phosphorylated Cx43 [39]. However, that antibody did not work well in immunoprecipitation or immunofluorescence experiments [40], possibly indicating distinct biochemical properties from those of CT1.

These results are consistent with evidence that phosphorylation could play a role in regulating Cx43 transport from ER to Golgi, to TGN, to plasma membrane, to gap-junction plaques and internalization. The C-terminus of Cx43 contains 21 serine residues, and to date, a total of twelve serine residues and two tyrosine residues have been reported to be phosphorylated following stimulation of various kinases (reviewed in [41]). For example, PKC (protein kinase C) phosphorylates residue Ser^{368} whereas MAPK (mitogen-activated protein kinase) phosphorylation occurs at Ser^{255}, Ser^{279} and Ser^{282} of Cx43 and causes distinct changes in the gating properties of gap-junctional channels [42,43]. Phosphorylation events at Ser^{325}, Ser^{328} and/or Ser^{330} are correlated with the regulation of gap junction assembly [44] and Ser^{364} phosphorylation plays a role in enhanced gap junction assembly [35]. Ser^{365} has been shown to be phosphorylated in response to follicle-stimulating hormone partially through a PKA (protein kinase A)-mediated mechanism [36,37]. Phosphorylation of specific serine residues has also been shown to be regulated in the heart. Notably, Ser^{364} is the start of a tandem repeat of Arg–X–Ser–Ser–Arg found in amino acids 362–374 and a naturally occurring S364P mutation reported in visceroatrial heterotaxia [45] that in experimental model systems can cause alteration of gating or expression [46,47]. A hypoxia model of ischaemia has shown regulation of specific phosphorylation sites including an increase in PKC-mediated phosphorylation on Ser^{368} [18] and a decrease in phosphorylation on Ser^{325}/Ser^{328}/Ser^{330} [16]. In the present study we show that the CT1 epitope increases upon hypoxia consistent with increases in Ser^{368}, and is negatively correlated with Ser^{325}/Ser^{328}/Ser^{330} phosphorylation and retention of Cx43 in gap-junction plaques.

Since the same 23 amino acid peptide was able to generate two conformationally distinct paratopes, the C-terminus has the potential to sense and transduce important and specific information via conformational changes. NMR analysis of small soluble domains of connexin peptides in solution has provided insights into the cytoplasmic structure that in general appears to be highly disordered (see the recent review in reference [48]). The structure of a large portion of the Cx43CT domain (amino acids 254–382, Figure 9) shows one α-helix at segment Ala^{311}–Ser^{325} and possibly another at Asp^{339}–Lys^{345}. Even with acidification, there are only minor changes, resulting in a slight decrease in α helicity at the N-terminus, and an increase at the C-terminus of the peptide [33,49] although there is a dimerization of the C-terminal peptide seen at low pH. The C-α backbone of the 254–382 amino acid peptide as determined by solution structure NMR is shown in Figure 9. In this Richardson diagram, the positions of all serine residues are marked in white. With the exception of Ser^{325}, all other serine residues map on to unordered regions of sequence. Ser^{325} is found at the end of one of the two short helices. The flexibility of the C-terminus may serve a purpose in being able to rapidly adapt locally new conformations upon phosphorylation, dephosphorylation or changes in interacting partners. The ability of both CT1 and IF1 to recognize a conformational change implies that a physical change occurs to provide a suitable shape with which other connexin-interacting proteins can perform lock-and-key or induced-fit mechanisms. Dynamic changes in the interactions of Cx43 with specific chaperone proteins that occur during the different steps in trafficking of the protein through its life cycle would fit with our working hypothesis that the conformation of the C-terminal

region of Cx43 regulates its exit from the Golgi apparatus and the stability of a gap junction.

Dr Paul Sorgen (University of Nebraska Medical Center, Omaha, Nebraska, U.S.A.) kindly provided the NMR co-ordinates for the C-terminus peptide solution structure. Dr Steven Taffet (Upstate Medical University, SUNY, Syracuse, NY, U.S.A.) generously provided some of the GST–Cx43CT deletion constructs. We thank Dr Ben Giepmans for advice, Galen Hand and Lucy Ngan for technical assistance in the early stages of this project and Joshua Brown for his help with Figure 9. Support was contributed by National Science Foundation grant MCB0543934 (to G. E. S.), National Institutes of Health grants GM55632 (to P. D. L.), GM072881 (to G. E. S.) and GM065937 (to G. E. S.). Some of the work included in the present study was conducted at the National Center for Microscopy and Imaging Research at San Diego, which is supported by National Institutes of Health Grant RR04050 awarded to Dr Mark Ellisman.

REFERENCES

1 Musil, L. S., Le, A.-C. N., VanSlyke, J. K. and Roberts, L. M. (2000) Regulation of connexin degradation as a mechanism to increase gap junction assembly and function. J. Biol. Chem. **275**, 25207–25215
2 Bennett, M. V. L. and Abrams, C. K. (2000) Hereditary human diseases caused by connexin mutations, In Gap Junctions. Molecular Basis of Cell Communication in Health and Disease (Peracchia, C., ed.). pp. 423–459, Academic Press, San Diego
3 Gerido, D. A. and White, T. W. (2004) Connexin disorders of the ear, skin, and lens. Biochim. Biophys. Acta **1662**, 159–170
4 Rabionet, R., Lopez-Bigas, N., Arbones, M. L. and Estivill, X. (2002) Connexin mutations in hearing loss, dermatological and neurological disorders. Trends Mol. Med. **8**, 205–212
5 Dêschenes, S. M., Walcott, J. L., Wexler, T. L., Scherer, S. S. and Fischbeck, K. H. (1997) Altered trafficking of mutant connexin32. J. Neurosci. **17**, 9077–9084
6 Laird, D. W. (1996) The life cycle of a connexin: gap junction formation, removal, and degradation. J. Bioener. Biomembr. **28**, 311–318
7 Bukauskas, F. F., Jordan, K., Bukauskiene, A., Bennett, M. V. L., Lampe, P. D., Laird, D. W. and Verselis, V. K. (2000) Clustering of connexin43-enhanced green fluorescent protein gap junction channels and functional coupling in living cells. Proc. Natl. Acad. Sci. U.S.A. **97**, 2556–2561
8 Musil, L. M. and Goodenough, D. A. (1993) Multisubunit assembly of an integral plasma membrane channel protein, gap junction connexin43, occurs after exit from the ER. Cell **74**, 1065–1077
9 Gaietta, G., Deerinck, T. J., Adams, S. R., Bouwer, J., Tour, O., Laird, D. W., Sosinsky, G. E., Tsien, R. Y. and Ellisman, M. H. (2002) Multicolor and electron microscopic imaging of connexin trafficking. Science **296**, 503–507
10 Lauf, U., Giepmans, B. N., Lopez, P., Braconnot, S., Chen, S. C. and Falk, M. M. (2002) Dynamic trafficking and delivery of connexons to the plasma membrane and accretion to gap junctions in living cells. Proc. Natl. Acad. Sci. U.S.A. **99**, 10446–10451
11 Thomas, T., Jordan, K. and Laird, D. W. (2001) Role of cytoskeletal elements in the recruitment of Cx43-GFP and Cx26- YFP into gap junctions. Cell Commun. Adhes. **8**, 231–236
12 Laird, D. W., Castillo, M. and Kasprzak, L. (1995) Gap junction turnover, intracellular trafficking, and phosphorylation of connexin43 in brefeldin A-treated rat mammary tumor cells. J. Cell Biol. **131**, 1193–1203
13 Shaw, R. M., Fay, A. J., Puthenveedu, M. A., von Zastrow, M., Jan, Y. N. and Jan, L. Y. (2007) Microtubule plus-end-tracking proteins target gap junctions directly from the cell interior to adherens junctions. Cell **128**, 547–560
14 Musil, L. S., Cunningham, B. A., Edelman, G. M. and Goodenough, D. A. (1990) Differential phosphorylation of the gap junction protein connexin43 in junctional communication-competent and -deficient cell lines. J. Cell Biol. **111**, 2077–2088
15 Musil, L. S. and Goodenough, D. A. (1991) Biochemical analysis of connexin43 intracellular transport, phosphorylation, and assembly into gap junctional plaques. J. Cell Biol. **1991**, 1357–1374
16 Lampe, P. D., Cooper, C. D., King, T. J. and Burt, J. M. (2006) Analysis of connexin43 phosphorylated at S325, S328 and S330 in normoxic and ischemic heart. J. Cell Sci. **119**, 3435–3442
17 Solan, J. L., Fry, M. D., TenBroek, E. M. and Lampe, P. D. (2003) Connexin43 phosphorylation at S368 is acute during S and G2/M and in response to protein kinase C activation. J. Cell Sci. **116**, 2203–2211
18 Ek-Vitorin, J. F., King, T. J., Heyman, N. S., Lampe, P. D. and Burt, J. M. (2006) Selectivity of connexin 43 channels is regulated through protein kinase C-dependent phosphorylation. Circ. Res. **98**, 1498–1505
19 Schoenenberger, C. A., Buchmeier, S., Boerries, M., Sutterlin, R., Aebi, U. and Jockusch, B. M. (2005) Conformation-specific antibodies reveal distinct actin structures in the nucleus and the cytoplasm. J. Struct. Biol. **152**, 157–168
20 Singh, D., Solan, J. L., Taffet, S. M., Javier, R. and Lampe, P. D. (2005) Connexin 43 interacts with zona occludens-1 and -2 proteins in a cell cycle stage-specific manner. J. Biol. Chem. **280**, 30416–30421
21 Hand, G. M., Martone, M. E., Stelljes, A., Ellisman, M. H. and Sosinsky, G. E. (2001) Specific labeling of connexin43 in NRK cells using tyramide-based signal amplification and fluorescence photooxidation. Microsc. Res. Tech. **52**, 331–343
22 Gaietta, G. M., Yoder, E. J., Deerinck, T., Kinder, K., Hanono, A., Han, A., Wu, C. and Ellisman, M. H. (2003) 5-HT2a receptors in rat sciatic nerves and Schwann cell cultures. J. Neurocytol. **32**, 373–380
23 Giepmans, B. N., Deerinck, T. J., Smarr, B. L., Jones, Y. Z. and Ellisman, M. H. (2005) Correlated light and electron microscopic imaging of multiple endogenous proteins using Quantum dots. Nat. Methods **2**, 743–749
24 Linstedt, A. D. and Hauri, H. P. (1993) Giantin, a novel conserved Golgi membrane protein containing a cytoplasmic domain of at least 350 kDa. Mol. Biol. Cell **4**, 679–693
25 Sonnichsen, B., Lowe, M., Levine, T., Jamsa, E., Dirac-Svejstrup, B. and Warren, G. (1998) A role for giantin in docking COPI vesicles to Golgi membranes. J. Cell Biol. **140**, 1013–1021
26 Sosinsky, G. E., Giepmans, B. N. G., Deerinck, T. J., Gaietta, G. M. and Ellisman, M. H. (2007) Markers for correlated light and electron microscopy. In Cellular Electron Microscopy (McIntosh, J. R., ed.). pp. 573–589, Elsevier, San Diego, CA
27 Jordan, K., Solan, J. L., Dominguez, M., Sia, M., Hand, A., Lampe, P. D. and Laird, D. W. (1999) Trafficking, assembly, and function of a connexin43-green fluorescent protein chimera in live mammalian cells. Mol. Biol. Cell **10**, 2033–2050
28 Giepmans, B. N. G. and Moolenar, W. H. (1998) The gap junction protein connexin43 interacts with the second PDZ domains of the zona occludins-1 protein. Curr. Biol. **8**, 931–934
29 Toyofuku, T., Yabuki, M., Otsu, K., Kuzuya, T., Hori, M. and Tada, M. (1998) Direct association of the gap junction protein connexin-43 with Z0–1 in cardiac myocytes. J. Biol. Chem. **273**, 12725–12731
30 Hunter, A. W., Barker, R. J., Zhu, C. and Gourdie, R. G. (2005) Zonula occludens-1 alters connexin43 gap junction size and organization by influencing channel accretion. Mol. Biol. Cell **16**, 5686–5698
31 Giepmans, B. N., Verlaan, I., Hengeveld, T., Janssen, H., Calafat, J., Falk, M. M. and Moolenaar, W. H. (2001) Gap junction protein connexin-43 interacts directly with microtubules. Curr. Biol. **11**, 1364–1368
32 Duffy, H. S., Sorgen, P. L., Girvin, M. E., O'Donnell, P., Coombs, W., Taffet, S. M., Delmar, M. and Spray, D. C. (2002) pH-dependent intramolecular binding and structure involving Cx43 cytoplasmic domains. J. Biol. Chem. **277**, 36706–36714
33 Sorgen, P. L., Duffy, H. S., Cahill, S. M., Coombs, W., Spray, D. C., Delmar, M. and Girvin, M. E. (2002) Sequence-specific resonance assignment of the carboxyl terminal domain of Connexin43. J. Biomol. NMR **23**, 245–246
34 Shibayama, J., Lewandowski, R., Kieken, F., Coombs, W., Shah, S., Sorgen, P. L., Taffet, S. M. and Delmar, M. (2006) Identification of a novel peptide that interferes with the chemical regulation of connexin43. Circ. Res. **98**, 1365–1372
35 TenBroek, E. M., Lampe, P. D., Solan, J. L., Reynhout, J. K. and Johnson, R. G. (2001) Ser364 of connexin43 and the upregulation of gap junction assembly by cAMP. J. Cell Biol. **155**, 1307–1318
36 Yogo, K., Ogawa, T., Akiyama, M., Ishida, N. and Takeya, T. (2002) Identification and functional analysis of novel phosphorylation sites in Cx43 in rat primary granulosa cells. FEBS Lett. **531**, 132–136
37 Yogo, K., Ogawa, T., Akiyama, M., Ishida-Kitagawa, N., Sasada, H., Sato, E. and Takeya, T. (2006) PKA implicated in the phosphorylation of Cx43 induced by stimulation with FSH in rat granulosa cells. J. Reprod. Dev. **52**, 321–328
38 Puranam, K. L., Laird, D. W. and Revel, J.-P. (1993) Trapping an intermediate form of connexin43 in the Golgi. Exp. Cell Res. **206**, 85–92
39 Nagy, J. I., Li, W. E. I., Roy, C., Doble, B. W., Gilchrist, J. S., Kardami, E. and Hertzberg, E. L. (1997) Selective monoclonal antibody recognition and cellular localization of an unphosphorylated form of connexin43. Exp. Cell Res. **236**, 127–136
40 Cruciani, V. and Mikalsen, S. O. (1999) Stimulated phosphorylation of intracellular connexin43. Exp. Cell Res. **251**, 285–298
41 Solan, J. L. and Lampe, P. D. (2005) Connexin phosphorylation as a regulatory event linked to gap junction channel assembly. Biochim. Biophys. Acta **1711**, 154–163
42 Lampe, P. D., TenBroek, E. M., Burt, J. M., Kurata, W. E., Johnson, R. G. and Lau, A. F. (2000) Phosphorylation of connexin43 on serine368 by protein kinase C regulates gap junctional communication. J. Cell Biol. **149**, 1503–1512
43 Warn-Cramer, B. J., Lampe, P. D., Kurata, W. E., Kanemitsu, M. Y., Loo, L. W., Eckhart, W. and Lau, A. F. (1996) Characterization of the mitogen-activated protein kinase phosphorylation sites on the connexin-43 gap junction protein. J. Biol. Chem. **271**, 3779–3786
44 Cooper, C. D. and Lampe, P. D. (2002) Casein kinase 1 regulates connexin-43 gap junction assembly. J. Biol. Chem. **277**, 44962–44968

45 Britz-Cunningham, S. H., Shah, M. M., Zuppan, C. W. and Fletcher, W. H. (1995) Mutations of the connexin43 gap junction gene in patients with heart malformations and defects in laterality. New Engl. J. Med. **332**, 1323–1329
46 Ek-Vitorin, J. F., Calero, G., Morley, G. E., Coombs, W., Taffet, S. M. and Delmar, M. (1996) pH regulation of connexin43: molecular analysis of the gating particle. Biophys. J. **71**, 1273–1284
47 Levin, M. and Mercola, M. (1998) Gap junctions are involved in the early generation of left-right asymmetry. Dev. Biol. **203**, 90–105
48 Sosinsky, G. E. and Nicholson, B. J. (2005) Structural organization of gap junction channels. Biochim. Biophys. Acta **1711**, 99–125
49 Sorgen, P. L., Duffy, H. S., Spray, D. C. and Delmar, M. (2004) pH-dependent dimerization of the carboxyl terminal domain of Cx43. Biophys. J. **87**, 574–581

Received 23 April 2007/13 August 2007; accepted 23 August 2007
Published as BJ Immediate Publication 23 August 2007, doi:10.1042/BJ20070550